2016-01-8099
Published 09/27/2016

doi:10.4271/2016-01-8099
saecomveh.saejournals.org

Dynamic Analysis of the Lubrication in a Wet Clutch of a Hydromechanical Variable Transmission

Andrea Bassi, Massimo Milani, Luca Montorsi, and Stefano Terzi
Universita di Modena e Reggio Emilia

ABSTRACT

The paper investigates the oil flow through a multi plate clutch for a hydro-mechanical variable transmission under actual operating conditions. The analysis focuses on the numerical approach for the accurate prediction of the transient behavior of the lubrication in the gear region: the trade-off between prediction capabilities of the numerical model and computational effort is addressed. The numerical simulation includes the full 3D geometry of the clutch and the VOF multi-phase approach is used to calculate the oil distribution in the clutch region under different relative rotating velocities. Furthermore, the lubrication of the friction disks is calculated for different clutch actuation conditions, i.e. not-engaged and engaged positions. The influence of different geometrical features of the clutch lubricating circuit on the oil distribution is also determined. The results show the areas where poor lubrication occurs and extend the experiments where measurements are difficult to carry out. The simulation highlight the regions where high thermal stresses are observed during tests.

CITATION: Bassi, A., Milani, M., Montorsi, L., and Terzi, S., "Dynamic Analysis of the Lubrication in a Wet Clutch of a Hydromechanical Variable Transmission," *SAE Int. J. Commer. Veh.* 9(2):2016, doi:10.4271/2016-01-8099.

INTRODUCTION

Numerical analysis is gaining an important role in the design of hydraulic components and systems. In particular, multidimensional simulation is increasingly applied to the investigation of the fluid dynamics behavior of hydraulic systems in order to broaden and complete the experimental campaigns. Moreover, the human and computational resources to be involved in the numerical analysis are now not only acceptable, but also advantageous, due to the continuous development of computational platforms and CFD tools. Numerical modeling is particularly useful in analyzing the fluid dynamic behavior in regions where experimental measurements are very difficult or even impossible to carry out.

In this paper, the ATF (automatic transmission fluid) flow through a multi plate clutch of a hydro-mechanical variable transmission is investigated with a multi-phase multi component numerical analysis. The CFD tool enables simulation of the fluid dynamic behavior of the ATF, accounting for the real complex geometry of the clutch under actual operating conditions and configurations. Thus, the lubrication process can be addressed and critical geometrical features or not efficient oil distribution outlined. Experimental investigation of simplified systems is possible with transparent components and modern acquiring techniques; for instance, in [1] the air velocity profile between rotating disks made of transparent polycarbonate has been measured using laser-Doppler anemometry. In [2] the application of the fast image processing was adopted for the characterization of a multiphase flow through transparent polymethyl-methacrylate prototypes. Indeed, the experimental approaches are very difficult to employ when analyzing the full physics of the lubrication within a multi plate clutch, including not only a complex geometry, but also a multiphase flow, high friction and structural stresses and high rotating speeds.

In literature, there are many examples that prove the reliability of the numerical modeling for the simulation of multi-phase flows by comparing the calculations to experimental values. For instance, in [3] a CFD multiphase analysis was implemented in order to study the cavitation phenomena in hydraulic components and the results were validated against experimental measurements available in literature. Similar approach was adopted in [4] and [5] for evaluating the multi-phase flow in a directional control valve for load sensing application and in a closed center load-sensing proportional control valve respectively. Though, complex physics including multi-phase and multi-components phenomena can be addressed [6], only recently CFD modeling has been employed in the analysis of the ATF flow through the plates of a wet clutch. In [7] the multidimensional simulation was adopted for investigating the multiphase flow through an open grooved two-disc system, but a single phase and constant flow inlet boundary were assumed, while in the real phenomenon each couple of plates has a non-uniform air-oil mixture and pressure distribution at the boundaries. In this paper, the whole clutch geometry has been considered and the oil distribution to each plate has been predicted as a function of the component design and operating conditions. In fact, the flow distribution has a fundamental role for the heat dissipation and wear out of the friction plates. Different numerical methods have been proposed for the wear prediction considering thermal degradation as in [8] and [9]. Furthermore, in [10] the thermal aspects of the engagement process

in a wet clutch have been also investigated numerically. Since it is very difficult to assess the oil distribution between the plates, heavy assumptions have been made; as in [8] where the ATF is assumed to completely fill the plates' clearance, even though the same authors suggested that indeed the ATF film fills the clearance only partially at high rotating speeds, especially for the friction plates with grooves. Furthermore, the flow through the clutch plates is not only a multi-phase mixture, but it is also turbulent as determined in [7] and [11]. In this paper, a turbulent flow has been considered and the k-ε turbulence model was adopted due to its good tradeoff between accuracy and numerical stability as demonstrated in [12].

Multi plate wet clutches are widely employed in powertrains where high-energy transmission and durability of the friction material are required. The lubrication process is crucial to prevent the degradation of the friction material, reducing the wear behavior. For this reason, the design of the clutch lubrication layout is important in order to distribute adequately the ATF to the plates. A simulation of the complete geometry has been implemented in order to study the fluid dynamic behavior of the ATF in the entire geometry and in particular on the plates' surfaces. The results obtained from the entire geometry have been compared to the values that can be achieved by a simplified geometry that provides similar accuracy but it is characterized by a much lower computational effort and calculation time. Using the simplified model, it is possible to study the oil flow field for different operating conditions and configurations of the clutch, i.e. disengaged and engaged clutch. The calculation of oil distribution for each plate identifies the regions where a poor lubrication may cause failures or fast wear out of the disks. The numerical results are compared to the plates' conditions at the end of a real clutch test.

CASE TEST

The clutch object of this study is shown in Figure 1 and represents a classic architecture of a wet clutch. The analyzed geometry of the clutch includes the following elements: the shaft, the return spring, the gear, the piston, the steel plates, the friction plates and the clutch housing. The friction plates are connected to the gear, while the other components to the shaft. The void volume in this region represents the fluid domain where the oil flows for lubricating and cooling the different parts. Even though the geometry is essentially cyclic, due to the different rotation speeds of the gear and the shaft before engagement the fluid dynamics problem is fully three dimensional and no symmetry boundaries can be adopted to simplify the domain.

The lubrication oil reaches the clutch through the duct realized in the shaft from the main lubricating circuit. A single inlet duct supplies the ATF to the gear internal chamber, which is the main responsibility of the ATF distribution to the plates region. In the gear chamber, a multi-phase flow develops since the ATF mixes with the air inside the clutch. The holes realized on the gear (GHs) distribute the ATF to the plates' regions. The ATF can also reach the plates' regions through the lateral ring (LR), since its area is relevant. The LR is the annular volume on the left of the Figure 2b. The oil distribution determines the inlet boundary conditions for the gaps between each steel plate and grooved plate. Therefore, the velocity field in the plates' clearance depends on the inlet conditions from the GHs as well as on the rotation speed of each plate. The ATF reaches the tank through the shaft holes (SHs) and the lateral outlet (LO). The tank pressure is assumed at atmospheric pressure.

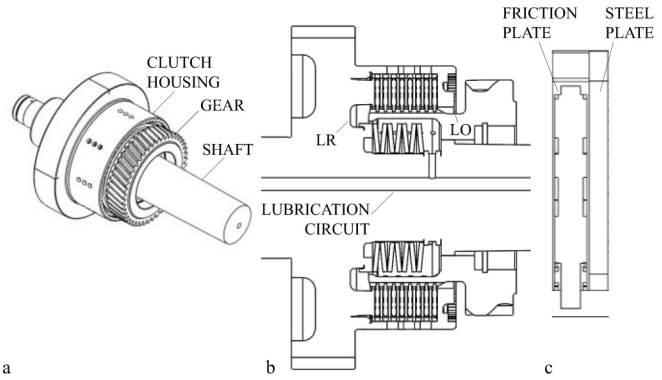

Figure 1. Schematic of (a) the wet clutch and (b) the lubrication circuit. (c) Zoom of a couple of steel and friction plates.

A typical engagement cycle for a wet clutch can be divided into four stages: *engagement, soaking, dwell and stabilization*. The engagement stage starts with the pressurization of the actuation cylinder chamber and ends when the relative speed between the steel and the friction plates becomes null. During this period, the clutch goes from the open configuration, where the clearance between the plates is maximum, to the closed configuration, where the zero gap is reached. The lubrication of the steel plates is extremely important during the engagement phase, since the maximum heat generation occurs and the high conductance of the steel plates allows the dissipation of most of the friction heat generated. Furthermore, during the engagement the oil on the steel surface permeates into the lining due to its porous structure. In addition, the ATF flow into the grooves of friction material also cools the interface temperature. The soaking stage initial condition is the end of the engagement period and it lasts until the pressure in the actuation chamber is released. During this period, the relative speed between the plates is null since the plates are locked. The soaking stage final condition overlaps the dwell stage initial condition, which ends when the gap between the plates is restored to the initial value. In the stabilization stage, the ATF flows through the clearance of the plates and cools down the clutch.

The most critical stage, in terms of heat exchange and temperature development, is the engagement period. For this reason, in this paper, the lubrication distribution is studied for two configurations and operating conditions close to the engagement stage. The numerical analysis addresses two relative rotation speeds for the gear and the shaft that are considered the most critical ones. In particular, in the first operation the gear rotates faster than the shaft, while in the second one the shaft rotation speed is only slightly larger than the angular velocity of the gear.

METHODOLOGY

The CFD analysis of the clutch is carried out by means of the computational fluid dynamics code Star-CCM+ [13], licensed by CD-Adapco.

The Volume Of Fluid (VOF) approach is adopted for the solution of the mass conservation and the momentum equations of the multiphase isothermal flow. Eulerian multiphase physics for the air and oil phases is defined. For the oil uncompressible flow is assumed and the density and viscous properties at 70°C are used in the calculation. The interface between the gaseous and liquid phase is accounted for by means of the interaction due to the liquid surface tension. In this analysis, the cavitation and aeration phenomenon are not included. The turbulent flow is solved by means a two equation approach and the k-epsilon turbulent model is adopted due to its good tradeoff between accuracy and numerical stability. Two-layer wall treatment is considered to address the wall flow behavior. Bounded central differencing is used for the discretization of the momentum, second-order scheme for subgrid kinetic energy, and the mixture fraction. The conservation equation for mass, momentum is solved simultaneously using a pseudo-time-marching approach The second-order implicit method is used for time integration scheme. Finally, the gravity contribution is included in the simulation and its effect on the flow field is considered.

The Figure 2a shows the lateral section of the domain used in the simulation for the open configuration. The section shows the number of domains in which the complete geometry is subdivided. The partition takes the different rotational speeds of the regions into account; thus, the proper angular velocity is set up to the regions rigidly connected to the gear and the shaft respectively. The partition of the entire domain into sub-domains enables to account effectively for modifications to the initial geometry, since only the sub-domain where the modification takes place has to be remeshed. The spring region is neglected, since it is assumed that the flow through its plates do not obstruct significantly the ATF flow.

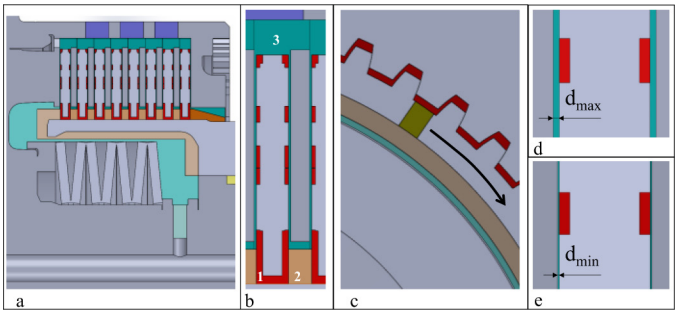

Figure 2. (a) Multicomponent domain for the simulation of the open configuration; (b) Modular approach, single reference unit; (c) tooth leakage due to gear and friction plate engagement; (d) open configuration; (e) closed configuration

The Figure 2b shows the modular approach for the computational domain of the plates' pack and the three repeated regions are highlighted with different colors: 1 - the groove region, 2 - the inner region and 3 - the steel plate region. In order to reconstruct the entire domain, the three regions are repeated 7 times. The last plate for the clutch housing is meshed separately, since it is slightly different from the other plates' regions. Further advantage of this meshing approach is the possibility of tailoring the mesh characteristics for each sub-domain thus improving the overall quality of the entire mesh.

The engagement region between the friction disk and the gear is accurately discretized in order to reproduce the leakage and the contact area due to the spin direction between the teeth, see Figure 2c. In fact, the leakage is an important feature to account for, since some GHs' outlet is located in front of the plate teeth and thus the oil would flow only through the leakage. Therefore, if no leakage is included those GHs would be obstructed.

Figure 2d and Figure 2e show the different gaps between two plates in the open and closed configurations, i.e. d_{max} and d_{min} respectively. In the closed configuration the considered clearance of the plates is assumed as the 25% of the gap in the open position ($d_{min} = 0.25\ d_{max}$).

In order to simulate the fluid dynamic behavior of the lubrication process in the complete geometry and in different operating conditions, two simulation strategies are implemented. The first one accounts for the entire domain and requires a remarkable computational effort; the second strategy adopts a simplified domain that is characterized by a lower computational effort and therefore it can be used for the simulation of different configurations.

The Figure 3 depicts the mesh of both the complete and the simplified geometry. In order to approximate the fluid dynamic behavior of the plates, the simplified geometry is cut where the grooves start. Since the grooves are the minimum cross section area and the pressure in these region is very close to the ambient value, as it will be shown in the results section, the geometry approximation does not affect remarkably the pressure distribution in the GHs' region. The meshing approach adopts a trimmed hexahedral discretization with a characteristic cell size in the order of 1 mm. Local cell refinements are employed for a better definition of the geometry features in particular regions, such as the plates' regions and the teeth leakages. A preliminary sensitivity analysis with respect to the mesh size was carried out in order to determine the best tradeoff between the accuracy of the results and the computational effort. The zoomed views of Figure 3b and c show the refinements in the plates' regions in the complete geometry; while the Figure 4b and c report the zooms in the plate regions in the open and closed configurations respectively. The number of cells of the complete geometry results 36.7 Million, instead the simplified geometry mesh amounts only to 14.1 Million cells. The number of cells for the open and closed configurations is similar since the hexahedral mesh can be resized non-uniformly along the three axes, thus preserving a minimum number of cells in the gap direction.

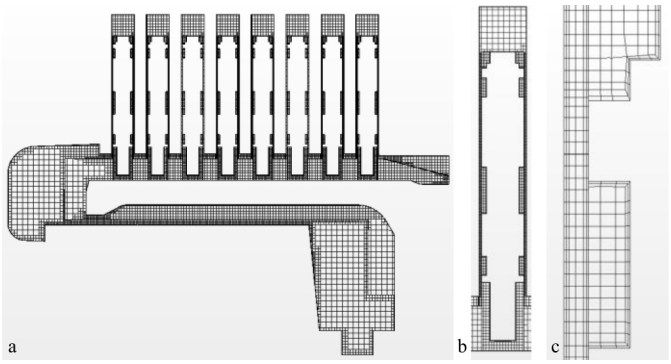

Figure 3. (a) Hexahedral mesh of the complete geometry. (b) and (c) zoomed views of the mesh in the plate regions.

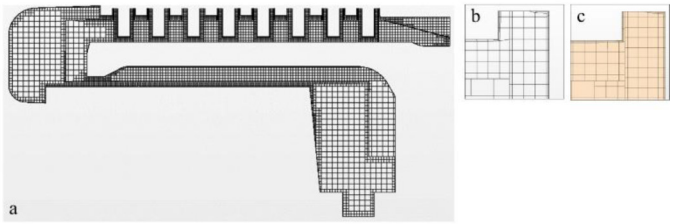

Figure 4. (a) Hexahedral mesh of the simplified geometry. (b) Zoomed view of the mesh in the plate region for the open configuration. (c) Zoomed view of the mesh in the plate region for the closed configuration

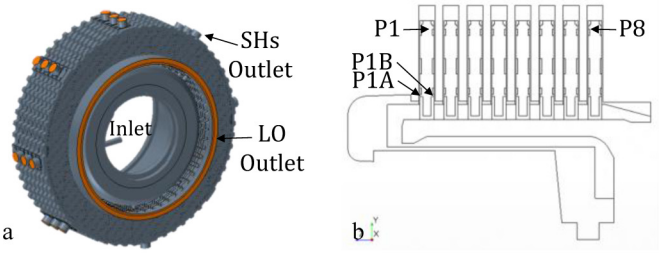

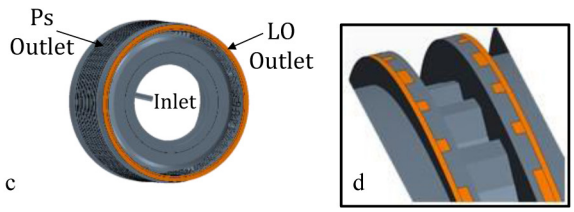

Figure 5. Boundary conditions (a) in the complete and (c) in the simplified geometries; (b) section of the complete geometry and (d) zoomed view of the clearance outlet boundary in the simplified geometry

Figure 5 outline the boundary conditions adopted in the simulations. The multiphase flow includes the uncompressible flow phases for air and oil. At the inlet boundary from the lubricating circuit, a constant mass flow rate of pure oil is set. The relating mass flow rate is determined by a preliminary CFD simulation of the entire lubrication circuit for the considered operating conditions. In particular, the measured values of the inlet mass flow rate and the pressure in several sections of the circuit were compared to the calculated ones. The comparison was carried out for different rotational speeds, since the inlet mass flow rates are different for the simulated operations due to the effect of the centrifugal forces. The outlet boundaries are different in the complete and in the simplified geometries. In the complete geometry, the outlets are real surfaces and correspond to the SHs and the LO outlet areas. These boundaries are set at ambient pressure since they are connected to the tank volume. The simplified geometry maintains the same pressure outlet condition in the LO and atmospheric pressure is set for the plates.

The rotation speed rates are hold constant during each simulation and different values are set for the gear and the shaft regions. In the complete geometry, a particular wall boundary velocity is used in the plate region to simulate the different rotation speed between the friction disk and the plate. Sliding interfaces are employed between gear and shaft regions in order to allow the fluid exchange in adjacent regions characterized by different rotations.

Table 1 summarizes the main characteristics of the simulations accounted for in this analysis. In particular, the boundary condition, the fluid properties and the angular velocity are highlighted. Table 2 details the shaft and the gear rotational speeds in the two operating conditions. Only the case #0 simulates the complete geometry (Comp.), while for the other cases the simplified geometry (Simpl.) is adopted. A fully transient approach is employed to simulate the filling of the clutch with the lubricating oil. Different simulation durations are adopted for the different cases in order to reach a stable condition of the flow. The time step for the implicit unsteady solver is selected accordingly to the simulated set of angular velocities in order to be shorter than the time required to sweep one degree for the fastest region (e.g. a time step equal to 6.43E-05s is adopted for the first velocity set and equal to 1.04E-04s for the second one).

Table 1. Main characteristics of the simulations.

Case #	Geom.	Set of velocities	Clutch Status	Q_{in} [l/min]	Clearance [mm]	T [°C]
0	Comp.	1	Open	Q_{ref}	d_{max}	70
1	Simpl.	1	Open	Q_{ref}	d_{max}	70
2	Simpl.	1	Closed	Q_{ref}	d_{min}	70
3	Simpl.	2	Open	0.9318 Q_{ref}	d_{max}	70
4	Simpl.	2	Closed	0.9328 Q_{ref}	d_{min}	70

Table 2. Speed rotation of the shaft and the gear regions.

Set of velocities	n_{shaft} [rpm]	n_{gear} [rpm]
1	1240	2590
2	1600	1500

RESULTS

The results of the simulations carried out on the complete geometry and on the simplified domain are described in the following paragraphs and the accuracy of the calculations obtained by means of the two approaches is compared. In the case of the entire geometry simulation, the results in terms of oil distribution are compared to the plates' conditions at the end of a real clutch test. Afterward, the effects on the oil distribution of different operating conditions and clutch engagement are investigated using the simplified geometry.

Complete Geometry

In this paragraph, the main results obtained in the Case #0 are discussed. Figure 6 shows the convergence condition reached for the complete geometry. The figure plots the percentage flow rate signal measured through the SHs. It is possible to notice that after a transient phase representing the oil filling, the values reach a stable behavior and steady regime after approximately 0.7 s. During the filling phase, the oil accumulates in the domain cavities and can be released impulsively. When steady state condition is reached, the flow field stabilizes and oscillations become periodically.

Figure 7 reports the fraction of the oil phase distribution on the frontal section at the inlet duct at 1.0 s of simulation time. By observing the oil fraction field, several considerations about the fluid dynamics behavior of the ATF can be drawn. The inlet duct is completely full of oil phase and continuously supplies the gear chamber. This result confirms that the outlet boundary of the preliminary simulation of the entire lubricating circuit was set correctly and the centrifugal forces were properly accounted for. The gear chamber is characterized by two hydraulic phenomena: a thin film of oil forms on the inner wall of the gear and it increases into a sort of wake downstream of the inlet duct. This film plays an important role in the lubrication distribution since it distributes the oil to all the GHs. When the oil film reaches the end on the internal gear wall, it flows through the LR. The air - oil distribution at regime condition demonstrates that a multiphase approach is fundamental in order to simulate this kind of application since the air phase occupies a large part of the domain. Furthermore, it is possible to notice that the oil distribution on the surface of the steel plate is definitely not uniform and it is strongly affected by the inlet duct position.

Figure 8 depicts the oil profile in a section through the shaft axis, and for the selected simulation time, i.e. 1.0 s, the section does not include the inlet duct. Since the inlet duct is far from the considered section, the oil film is quite uniform in the shaft axis direction and its thickness increases from right to left due to the tangential forces on the ATF. The LR volume is characterized by an accumulated amount of oil, which supplies further the P1A. The thickness and the volume fraction of the ATF in the LR varies with the circumferential position as a consequence of the inlet duct position. Observing the oil mass fraction distribution among the plates, it is possible to qualitatively remark that the oil flow decreased moving from P1 to the P8. Figure 9 plots the lateral section through the GHs of the line A of the gear. In this figure, the oil film is perturbed by the inlet flow, which causes a dynamic behavior and modifies the film thickness. The figure shows that the conductance of the GHs of a line depends on their position and on the flow profile and the hole in front of the inlet duct is not characterized by the largest amount of oil. Furthermore, the presence of a plate at the outlet of a GHs' hole does not obstruct the flow and that demonstrates the importance of including the teeth leakage in the simulation as described in Figure 2c.

The flow rate through the GHs is fundamental for the correct clutch lubrication, thus the oil distribution among the holes is accurately investigated. Figure 10 plots the numerical results for line A in terms of the time history of the flow rates supplied by the holes of line A and the statistical values of the flow rate curves calculated for the time period when regime condition is reached. In order to better visualize the position of each hole with respect to the inlet duct, a cut view of the gear through the considered GHs hole line A is provided in the figure. From the cut view, it is also possible to outline that the position of the GHs' lines is cyclic, thus line A is in the same position as line E with respect to the inlet duct. The flow rate profiles of the five GHs of the line A result in a quite similar trend that looks periodic as a function of the relative rotation speeds. It can be notice that the peak values vary among them, but mostly important is that only the A5 trend goes to zero for a remarkable period of time. The different behavior of holes A5 and E5 can be explained by their axial position with respect to the inlet duct; in fact, they are the only holes located at the right hand side of the inlet and just at the fillet. This apparently small difference proves to be enough to cause a lack of flow for an important portion of the revolution of the gear. The impulsive behavior of the flow rates is due to the alignment of the inlet duct with the different lines of GHs. The histograms reported in Figure 10 (g), (h) and (i) highlight the statistical values of the flow rate curves. In particular, the mean flow rate values demonstrate to increase from hole A1 to A5 and the trend follows the variation of the oil thickness on the gear inner wall. The impulsive nature of the lubrication is confirmed by the values of both the standard deviation and amplitude, which are very similar to the mean data for the former and much larger for the latter. The flow follows the oscillation induced by the rotation of the inlet duct, which perturbs the film shape and generates an important ripple of the GHs' flow rate signals. When comparing two opposite GHs' lines, i.e. line A and E, the statistical values are very similar and confirm the cyclic behavior of the flow field within the gear volume.

Figure 11 and Figure 12 compare the numerical results in terms of oil distribution to the plates' conditions at the end of a real clutch test. In particular, Figure 11 shows the correlation between oil distribution supplied through the plates and effects of fatigue on the real clutch after the clutch test. The histogram demonstrates that numerical results predict a not uniform distribution of oil through the eight plates and the values calculated for P5 and P6 are the lower ones (with the exception of P8), while P1 is characterized by the maximum flow rate. It is interesting to remark that P5 and P6 are the plates aligned to the inlet duct and nonetheless they result poorly lubricated. Therefore, the gear geometry and the resulting tangential forces demonstrate to have a fundamental role in the distribution of the oil to the different plates and their contribution can be even more important than the position of the inlet duct. The result that the plates P5 and P6 have a scarce lubrication is also confirmed by the experiments. Indeed Figure 11 (b) shows that the plates P5 and P6 have endured higher thermal stresses when compared to the other plates of the clutch after the test. The low oil flow rate to the P8 is considered not critical, since this plate is connected to a large steel and the much larger mass of P8 compared to the other plates allows the heat to be dissipated more efficiently. On the other side of the gear, the plate P1 result to be over-lubricated due to the ATF flow through the LR. Since P1 has similar geometry as P8 the large oil flow is even less useful, since the heat is effectively dissipated by its large mass.

Figure 12 compares the calculated oil distribution and the experimental state on two different plates: plate P1A that is the least thermally stressed after the experimental clutch test and plate P6A that demonstrates to be the most thermally stressed plate. The simulation results prove that the ATF distribution on the P1A surface is not homogeneous but a significant amount of oil is distributed all over the plate, thus it can be assumed that the oil can remove the heat generated during the engagement phase and therefore preserve the plate surface treatment. Conversely, the ATF distribution calculated on the P6A surface is still not homogeneous but on a large part of the plate the amount of oil is close to zero and only in the portion of the surface aligned to the inlet duct the oil volume fraction becomes sufficient. The poor lubrication of the plate causes a poor cooling effect of the oil and thus a more serious thermal stress as proved by the picture of the plate after the experimental clutch test.

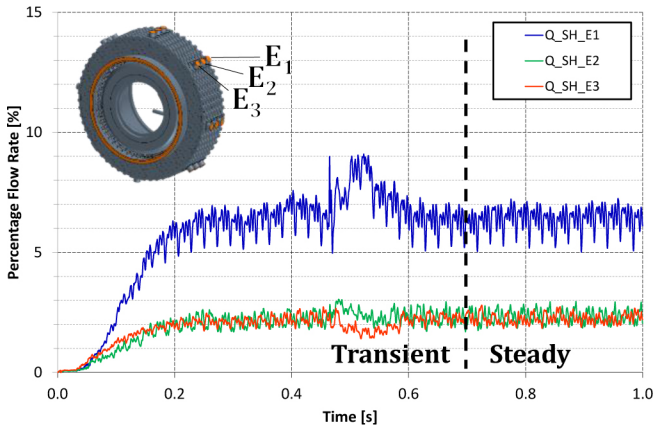

Figure 6. Stabilization of the flow rates after the clutch filling phase: percentage flow rate signal for the three SHs.

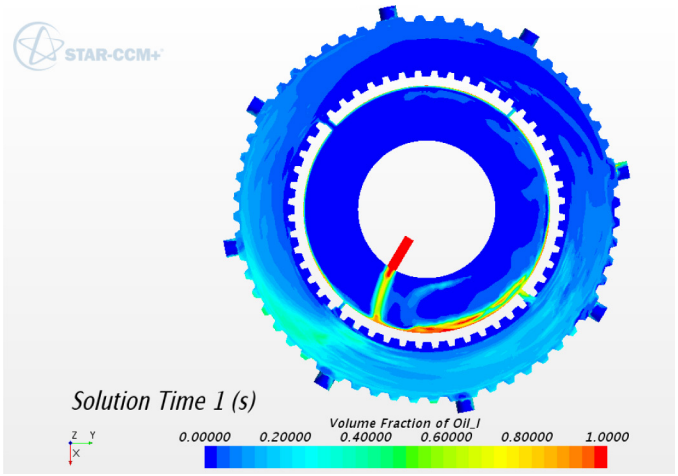

Figure 7. Oil distribution on the frontal section at the inlet duct at 1.0 s of simulation time.

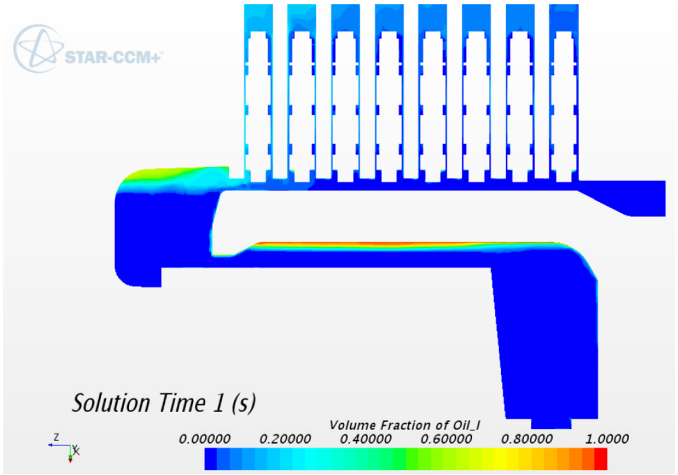

Figure 8. Oil distribution on a section through the shaft axis at 1 s simulation time (the section does not cut the inlet duct).

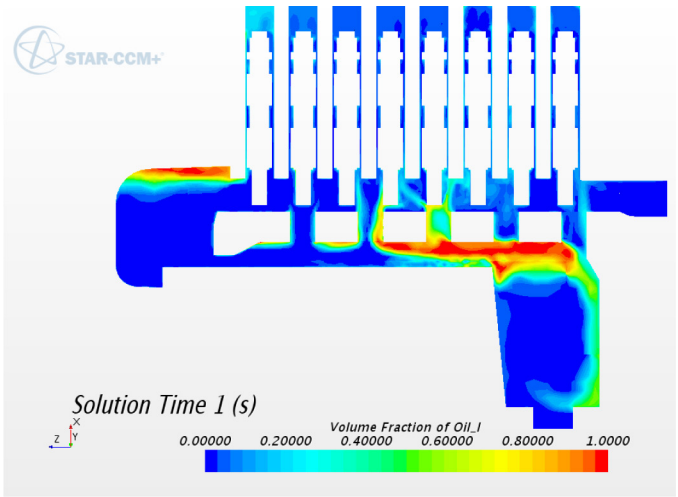

Figure 9. Oil distribution on lateral section through the GHs of the line A of the gear at 1.0 s simulation time.

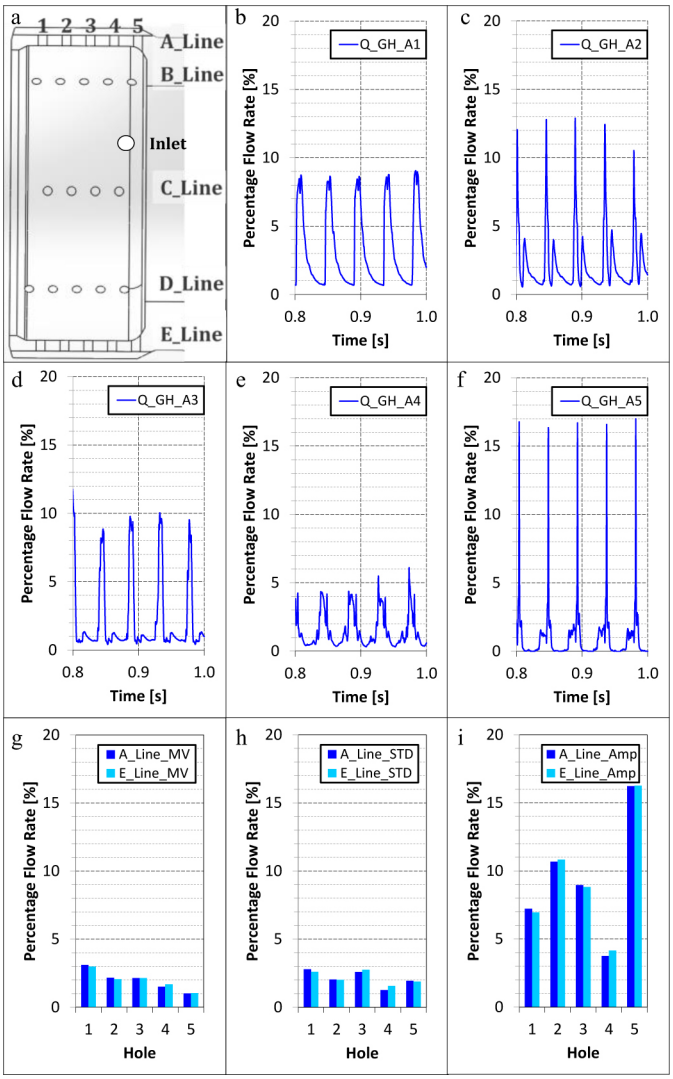

Figure 10. Characterization of the oil flow through the GHs of the A line. (a) Cut view of the gear through the GHs line A. From (b) to (f) the time history of the percentage flow rates supplied by the holes of line A from A1 to A5 and relative statistical values for the mean flow rate, the standard deviation and the amplitude for the holes of line A and E when regime condition is reached.

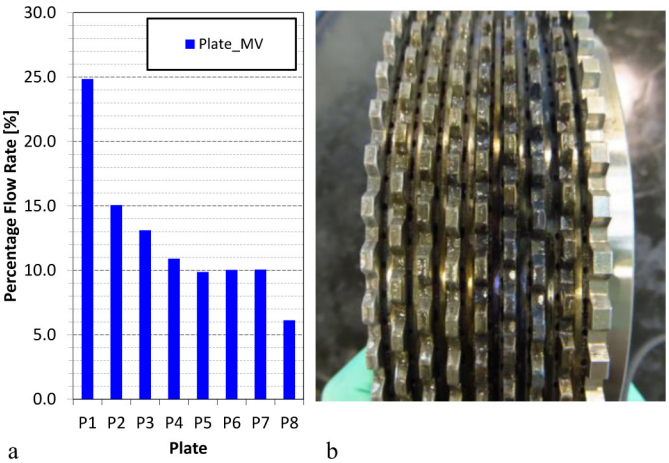

Figure 11. Correlation between calculated oil flow to the plates and plates' thermal stress on an experimentally tested clutch. (a) Oil percentage distribution to the plates and (b) Image of the experimentally tested clutch plates at the end of the clutch test.

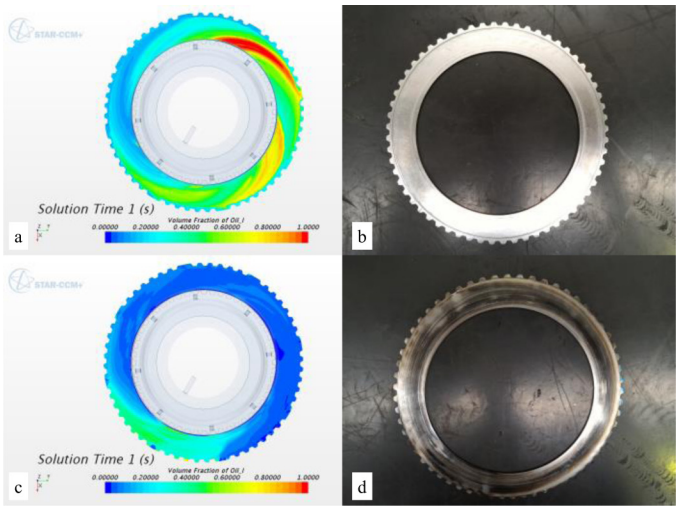

Figure 12. Correlation between simulated oil distribution and plates' thermal stress on an experimentally tested clutch for the plates (a) P1A and (b) P6A which proved to be the least and worst worn out respectively after the experimental clutch test.

Simplified Geometry

A critical issue of the numerical simulation presented in the previous paragraph is the computational effort and therefore the total simulation time. Therefore, a simplified approach for the clutch computational domain is proposed in order to have a faster computing model while maintaining a good accuracy in the oil flow distribution prediction. In this section, first the results of the full CFD domain, i.e. Case #0 of Table 1, are compared to the results obtained by the simplified fluid domain under the same operating conditions, i.e. Case #1. First, the oil filling transient and the flow stabilization time are addressed for the simplified geometry. Figure 13 reports the flow rates signals measured at the outlet of the first four plates that corresponds to the section where the grooves start and where the real geometry has been cut for simplifying the CFD domain. The selected plates are the farthest from the inlet duct and likely they are characterized by the longest stabilization time. The flow rate trends are similar to the outlet flow rate of the full geometry plotted in Figure 6. An initial oil filling phase can be observed and after 1.0 s the flow rates are completely stable and the regime condition is reached. The dynamics is very similar to the one predicted by the full geometry. Obviously, the values of the flow rate cannot be compared directly, in fact for the simplified geometry the flow rate is calculate for each plate, while in the full geometry, the outlet holes collect the flow from several plates.

Figure 14 reports the oil volume fraction distribution on a cut section through the inlet duct axis. The oil pattern results very similar to the one calculated by the full geometry case plotted in Figure 7. Thus, the simplified approach proves to be able to represent accurately the flow field within the gear chamber; in particular, the flow pattern from the inlet duct, the film dynamics in the inner wall of the gear and the oil accumulation regions are the same for the compared approaches.

Furthermore, by observing Figure 15 it can be concluded that the overall conductance of the full and simplified geometry is predicted to be very similar. In fact, the comparison of the average flow rates through the GHs and through each plate demonstrate a good agreement between Case # 0 and Case # 1. The two Cases calculate also the same flow rates for left and right sides of each plates, see Figure 16.

Therefore, the simplified domain approach proves to estimate accurately the results of the full geometry case. The lighter computational effort and the lower calculation times make it possible to effectively investigate a larger number of different operating conditions and configurations. In fact, the Case #0 requires 4 days of calculation time on a 32 processor parallel computer in order to simulate a single revolution of the gear region; while for Case #1 16 hours are enough to complete the revolution of the gear region on the same machine. Thus, the simplified geometry enables to cut the overall simulation time of approximately 6 times with respect to the full domain case.

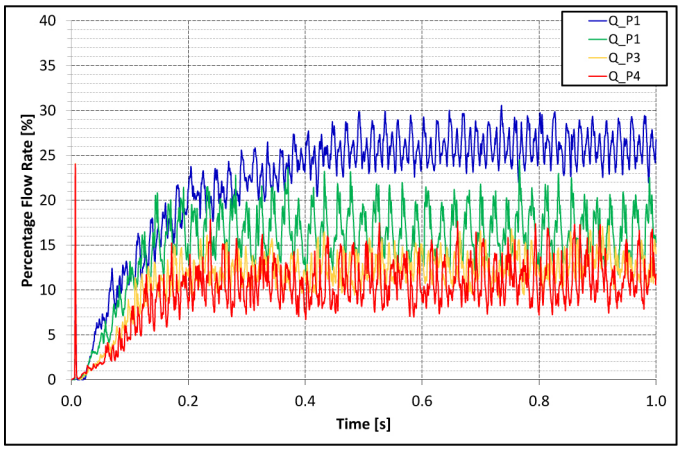

Figure 13. Stabilization of the flow rates after the clutch filling phase for the simplified geometry case: percentage flow rate signal through the first four plates.

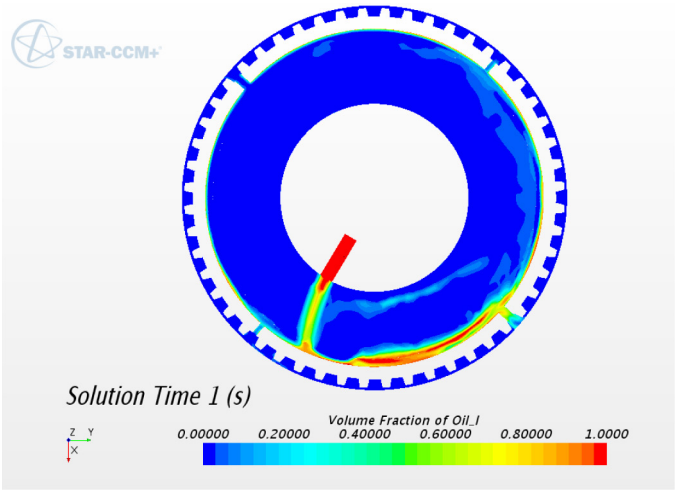

Figure 14. Volume fraction of oil in the frontal section at the inlet duct

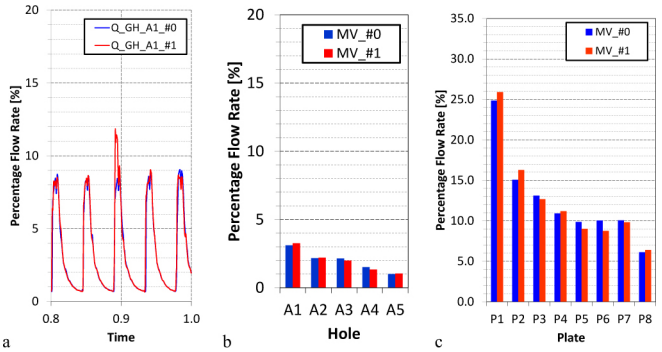

Figure 15. (a) Percentage flow rate measured through the GH_A1. (b) Percentage mean values of the flow rates calculated in the GHs of the A line. (c) Percentage mean values distribution of the flow rates calculated through the plates.

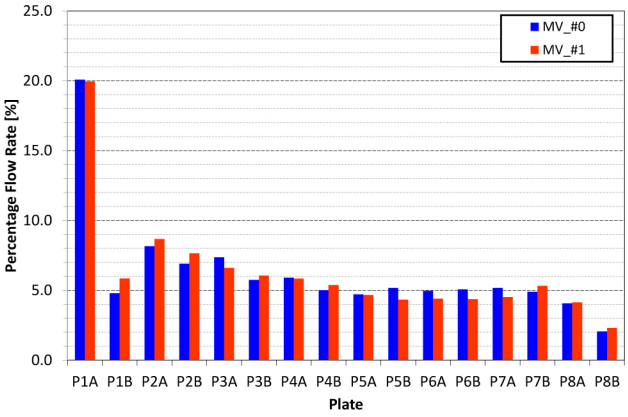

Figure 16. Percentage mean values calculated through the semi-plates

Influence of Operating Conditions and Clutch Position

Two relative rotation velocities of the gear and the shaft and two positions of the clutch plates are simulated in order to address their influence on the oil distribution, see Cases #1, #2, #3 and #4 of Table 1. In particular, the influence of the operating parameters is investigated in terms of flow field and oil flow rate distribution through the plates.

As mentioned in the previous section, the centrifugal forces and the wall viscous stresses due to the different rotations of the gear and the shaft play a fundamental role in determining the stabilized oil flow field and thus in the oil flux to the plates. Figure 17 shows the oil pattern for Case # 1 and # 3 on the frontal section at the inlet duct when fully stabilized flow regime is reached. It can be noticed that for the first set of angular velocities the film is thinner and oil accumulated downstream of the inlet duct is larger than for the second set of rotation speeds. In this case, the film thickness is higher all over the gear inner wall likely due to the lower centrifugal forces applies to the oil by the lower gear rotation; nevertheless, the height of the film results not uniform.

Figure 18 and Figure 19 compare the oil flow rate time history and the flow distribution through the plates for the disengaged and engaged position of the clutch rotating at the same speeds, i.e. the fastest set of velocities of Table 2. The dynamics of the flow looks very similar between the two analyzed configurations of the plates,

while the mean flow rates through each plate result more influenced by the plates' gaps and their relative position with the GHs. These features determine an increased flow through the first three plates and a reduction of the oil lubrication for P5, P6 and P7. This behavior can suggest a critical issue in the operation of the real clutch, since as mentioned before, P5 and P6 demonstrated to have the most thermally stressed.

The results of the second set of velocities, i.e. the slowest rotations, are presented in Figure 20 and Figure 21 for the disengaged and engaged positions. The time history flow rates of the gear hole A1 are still rather similar when considering the same set of velocities; while if they are compared to the faster set of velocities shown in Figure 18 a remarkable difference can be noticed. The peaks are reduced and in the case of the engaged position the flow goes close to zero in some instants of the revolution. When observing the mean flow rate through each plate, a lower difference between the values of the two plates' position can be noticed for the low rotations cases; nevertheless, the trend outlined for the previous set of velocities still holds and the first three plates result more lubricated for the engaged position to the detriment of P6 and P7.

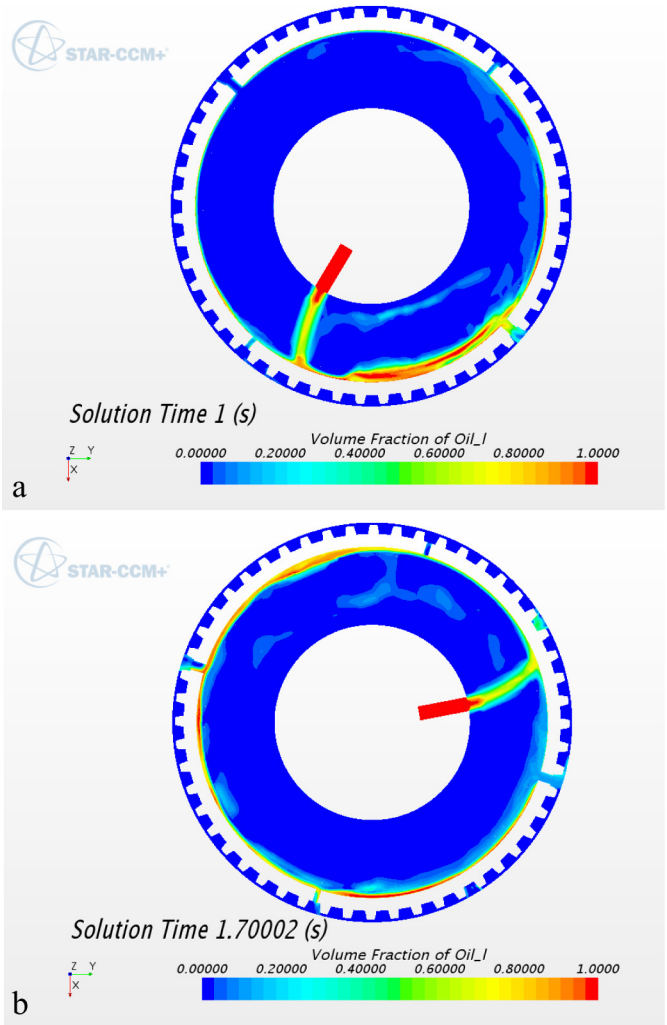

Figure 17. Oil distribution on the frontal section at the inlet duct when fully stabilized flow regime is reached for (a) Case #1 and (b) Case #3.

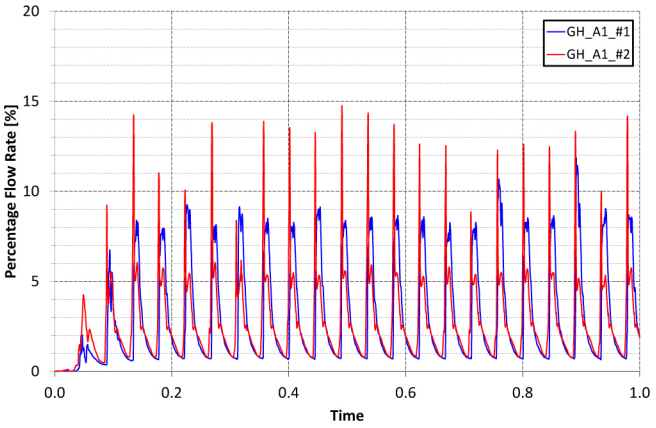

Figure 18. Comparison of the percentage flow rate time histories through the GH_A1 for the first set of rotational speeds in Case #1 and Case #2.

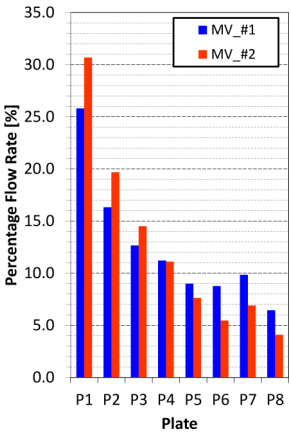

Figure 19. Percentage mean flow rates through each plate for the first set of rotational speeds in Case #1 and Case #2.

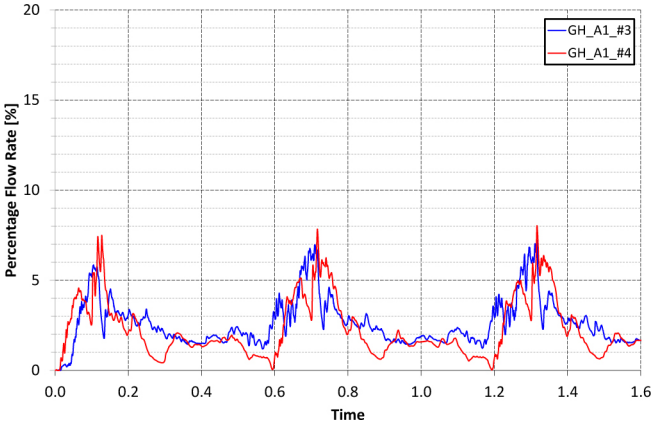

Figure 20. Comparison of the percentage flow rate time histories through the GH_A1 for the second set of rotational speeds in Case #3 and Case #4.

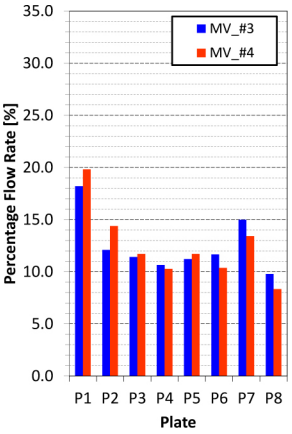

Figure 21. Percentage mean flow rates through each plate for the second set of rotational speeds in Case #3 and Case #4.

CONCLUSIONS

The CFD multi-phase simulation of the complete geometry of a multi-plate clutch was carried out under actual operating conditions. The VOF approach was adopted for modeling the oil - air mixing and the relative rotation speeds for the gear and the shaft were accounted for. The inlet flow rate was calculated by a previous simulation of the entire lubricating circuit in the same operating conditions as the analyzed clutch. Particular care was devoted in including the leakage between the teeth of the disks as well as the contact area of the teeth due to the engagement spin direction. The oil filling transient was simulated and the flow field within the gear region was investigated when a stable regime for the lubrication of the clutch was reached.

The numerical results of the complete geometry simulation provided an accurate analysis of the oil distribution in the entire clutch. The gear region demonstrated to be only partially filled with oil even when regime condition was fully met. A thin film formed at the inner surface of the gear due to the centrifugal forces and the wall viscous stress. It could be observed that a significant amount of oil accumulated downstream of the inlet duct. The flow through the gear holes demonstrated to be not uniform und unexpectedly the farthest holes from the inlet duct were characterized by the larger flow rates. Similarly, the flow through the plates of the clutch resulted very different and P5 and P6 were predicted to have the poorest lubrication.

The numerical oil distribution obtained with the complete geometry was compared to the plates' conditions at the end of a real clutch test. The comparison showed that the plates with the lowest calculated oil flow are the most worn out. In addition, the plates where the oil volume fraction is sufficient all over the surface do not present a significant thermal stress, while the plates where the oil film is predicted to be almost null demonstrated experimentally a more serious thermal stress after the clutch test.

Afterward, a simplified geometry was suggested in order to reduce the computational effort of the full geometry domain and the results obtained with the simplified approach were investigated to assess its accuracy. The simplified CFD domain demonstrated to predict the same oil flow distribution in the gear chamber and the average flow rates through the gear holes as well as through the clutch's plates resulted to be very close to the values calculated by the full geometry case. The simplified model enabled to reduce the computational time by a factor of six, thus enabling to investigate the influence on the oil lubrication of different rotational speeds and clutch configurations.

Finally, two sets of rotations and the disengaged and engaged configurations were simulated and compared. By observing the oil distribution in the gear chamber when fully stabilized flow regime is reached, the slower set of velocities was characterized by a larger film thickness in the inner wall of the gear with respect to the fastest set of rotations. This behavior was also confirmed by a more uniform distribution of the oil through the different plates in case of the slower set of rotations. When comparing the disengaged and engaged configurations by modifying the gap between the plates and thus the relative position of the GHs, the conductance of each plate changed and a different oil distribution was found. Nevertheless, for both geometries, the farthest plates from the inlet duct resulted more lubricated compared to the ones close to the oil supply duct. This behavior can suggest a critical issue in the operation of the real clutch, since the plates close to the inlet demonstrated experimentally to be the most thermally stressed.

REFERENCES

1. Gan, X.P. and Macgregor, S.A., "Experimental study of the flow in the cavity between rotating disks," Exp. Thermal Fluid Sci. 10 (3): 379-387, 1995, doi:10.1016/0894-1777(94)00099-T.
2. Bottazzi, D., Franzoni, F., Milani, M., and Montorsi, L., "Fast Image Processing Applied to Fluid Power Components," SAE Technical Paper 2009-01-2849, 2009, doi:10.4271/2009-01-2849.
3. Franzoni, F., Milani, M., and Montorsi, L., "Cavitating Flows in Hydraulic Multidimensional CFD Analysis," *SAE Int. J. Commer. Veh.* 1(1):424-436, 2009, doi:10.4271/2008-01-2678.
4. Bigliardi, E., Francia, M., Milani, M., Montorsi, L. et al., "Multiphase and Multi-component CFD Analysis of a Load - Sensing Proportional Control Valve" IFAC-PapersOnLine 48-1, 421-426, 2015, doi:10.1016/j.ifacol.2015.05.114.
5. Bottazzi, D., Franzoni, F., Milani, M., and Montorsi, L., "Metering Characteristics of a Closed Center Load - Sensing Proportional Control Valve," *SAE Int. J. Commer. Veh.* 2(2):66-74, 2010, doi:10.4271/2009-01-2850.
6. Lai, D., Milani, M., Montorsi, L., and Zoffoli, L., "Numerical analysis of the interaction between high-pressure resin spray and wood chips in a vapour stream" Advances in mechanical engineering 8: 1-13, 2016, doi: 10.1177/1687814016643243.
7. Hu, J., Wu, W., Xiong, Z. and Yuan, S., "Application of CFD to model oil-air flow in a grooved two-disc system" International Journal of Heat and Mass Transfer 91: 293-301, 2015, doi:10.1016/j.ijheatmasstransfer.2015.07.092.
8. Lam, R.C., and Yang, Y., "Theoretical and experimental studies on the interface phenomena during the engagement of automatic transmission clutch" Tribology Letters 5: 57-67, 1998, doi:10.1023/A:1019196331003.
9. Li, M., Khonsari, M.M., McCarthy, D.M.C. and Lundin, J., "On the wear prediction of the paper-based friction material in a wet clutch" Wear 334-335: 56-66, 2015, doi:10.1016/j.wear.2015.04.005.
10. Jang, J.Y. and Khonsari, M.M. "Thermal Characteristics of a Wet Clutch" J. Tribol 121(3): 610-617, 1999, doi:10.1115/1.2834111.
11. Eysion, A.L., James, H., Qian, Z. and Yuan, Y., "An Improved hydrodynamic model for open wet transmission clutches" J. Fluids Eng. 129 (3): 333-337, 2007, doi:10.1115/1.2427088.
12. Franzoni, F., Milani, M., and Montorsi, L., "A CFD Multidimensional Approach to Hydraulic Components Design," SAE Technical Paper 2007-01-4196, 2007, doi:10.4271/2007-01-4196.
13. CD-Adapco, 2015, Star-CCM+ 10.06.009 User Guide.

CONTACT INFORMATION

Prof. Ing. Massimo Milani, Ph.D.
DISMI, University of Modena and Reggio Emilia
Via Amendola 2 - Padiglione Morselli
42122, Reggio Emilia - ITALY
massimo.milani@unimore.it

Ing. Stefano Terzi, Ph.D. Student
DISMI, University of Modena and Reggio Emilia
Via Amendola 2 - Padiglione Morselli
42122, Reggio Emilia - ITALY
stefano.terzi@unimore.it

ACKNOWLEDGEMENTS

The authors would like to acknowledge Dana Rexroth Transmission Systems S.r.l. for supporting this work and particularly would like to thank Mr. Fabrizio Panizzolo, Mr. Giovanni Profumo, Mr. Stefano Mercati and Mr. Marcello Conatrali for their contribution.

DEFINITIONS/ABBREVIATIONS

Amp - Amplitude

ATF - Automatic transmission fluid

CFD - Computational Fluid Dynamics

$\mathbf{d_{max}}$ - Maximum gap between clutch plates

$\mathbf{d_{mim}}$ - Minimum gap between clutch plates

GH - Gear hole

GH_XY - Gear hole - X = Line [A; H] - Y = Column [1; 5]

LO - Lateral outlet

LR - Lateral ring

MV - Mean Value

$\mathbf{n_{gear}}$ - Rotation speed of the gear

$\mathbf{n_{shaft}}$ - Rotation speed of the shaft

P - Plate

PX - Plate - X = Plate [1; 8]

PXY - Plate: - X = Plate [1; 8] - Y = Side [A; B]

Q_GH_XY - Flow rate measured through the gear hole - X = Line [A; H] - Y = Column [1; 5]

Q_PX - Flow rate measured through the plate clearance - X = Plate [1; 8]

Q_SH_XY - Flow rate measured through the shaft hole - X = Line [A; H] - Y = Column [1; 3]

$\mathbf{Q_{in}}$ - Inlet flow rate

$\mathbf{Q_{ref}}$ - Reference inlet flow rate value

SH - Shaft hole

SH_XY - Shaft hole - X = Line [A; H] - Y = Column [1; 3]

STD - Standard Deviation

VOF - Volume of fluid